https://doi.org/10.37434/tpwj2021.12.03

CALCULATED-EXPERIMENTAL MODEL OF DISTRIBUTION OF NON-METALLIC INCLUSIONS IN THE METAL OF WELDS BY SIZES

L.A. Taraborkin, **V.V. Holovko**

E.O. Paton Electric Welding Institute of the NASU
11 Kazymyr Malevych Str., 03150, Kyiv, Ukraine

ABSTRACT

There is a large number of investigations on the impact of distribution of non-metallic inclusions in the weld metal on its structure and mechanical properties. However, the authors of these works do not describe the kinetics of forming such a distribution. The results of the development of a distribution model in the weld metal of non-metallic inclusions by sizes are presented. Formation of the calculation part of the model is based on the processing of experimental data on the sizes of non-metallic inclusions in the metal of welds, deposited by the methods of submerged arc welding and in shielding gas. Generalization and analysis of experimental data showed that the final distribution of inclusions in the metal of the studied welds is submitted to the law of gamma-distribution (probability is > 95 %). To describe the evolution of the distribution of non-metallic inclusions during weld formation, the authors proposed to apply a probabilistic model in the form of gamma-distribution with time-dependent parameters.

KEY WORDS: low-alloy steel, welding, weld metal, non-metallic inclusions, distribution

INTRODUCTION

Non-metallic inclusions are an integral component of the weld metal structure. Their characteristics such as chemical composition, sizes, distribution density in a solid solution have a significant impact on mechanical properties of weld metal, which determines the relevance of the possibility of their forecasting. In connection with the ever-increasing volume of low-alloy high-strength steels in the manufacture of metal structures, in recent years a lot of attention is paid to the study of the possibilities of providing mechanical properties of welded joints on steels of this type at the level of the base metal. A significant influence on the conditions for the microstructure formation and mechanical properties of weld metal from non-metallic inclusions was shown [1–4], that affect the processes of crystallization, formation of primary and secondary microstructure. But at the same time, in parallel, a change in the parameters of their size, distribution density, composition and surface compounds is observed. In the weld metal, the final result of the processes of forming non-metallic inclusions (deoxidation of liquid metal, crystallization of weld pool, diffusion in a solid solution) was recorded, which occurs in different temperature ranges. The intensity of the development of each of the stages of these processes affects the final distribution of non-metallic inclusions. Thus, for example, in [5] it was shown that the time of existing a liquid phase during cooling of the metal has a significant impact on the sizes of inclusions. Therefore, to predict the characteristics of inclusions, it is necessary to take into account not only the chemical composition of the weld pool, but also the time of its existence. It should be noted that despite a large number of works, in which the influence of the composition, morphology and sizes of non-metallic inclusions on the structure and mechanical properties of weld metal, insufficient attention was paid to the issue of the effect of the distribution of inclusions, depending on their size.

STATE-OF-THE-ART OF THE PROBLEM

The distribution of non-metallic inclusions in metals by sizes is numerically characterized by means of the function of the distribution density, which is generally determined by solving the Smoluchowski equation [6]. However, since the processes of coarsening non-metallic inclusions are rather complicated in any metallurgical system, then for such a solution it is necessary to introduce additional assumptions regarding the conditions and characteristics of the relevant process that are not always equipped with the necessary numerical values of parameters or not subjected to checking at all. For example, in the mentioned work [6], a list of the mentioned assumptions has 19 points. Therefore, another calculation and experimental approach is used, namely: based on a large array of accumulated experimental data, researchers are trying to approximate experimentally observed distributions of non-metallic inclusions by sizes by certain known mathematical functions of distributions.

In particular, in [7, 8] it is noted that distribution of non-metallic inclusions by sizes for some non-stationary metallurgical processes can be considered as a constant exponential distribution and described by the formula

$$n(r) = n_0 \exp(-\lambda r),\ r_0 < r < r_{\max}, \tag{1}$$

where the parameters n_0, λ depend on specific conditions and equipment, and inclusions have a shape of the sphere with the current radius r.

Formula (1) is suitable in the case of such metallurgical processes of steel production as a circulating vacuuming, vacuum refining, continuous pouring and ladle treatment. For these processes, the values λ are in the range from 0.44 to 0.75 for the radii of non-metallic inclusions from 1 to 30 μm [7].

It is known, that both the sizes of non-metallic inclusions themselves, as well as the density of their distribution by sizes depends on duration of the processes of inclusion formation [8–10].

The process of forming non-metallic inclusions in the welding pool is significantly different both as to its thermodynamic as well as to physico-chemical characteristics from the corresponding processes of a "large" metallurgy. Certain attempts on numerical evaluation of trends in changing the density of non-metallic inclusions depending on their sizes [11] can be noted, but in general, in scientific and technical literature, descriptions of models for calculating the distribution of inclusions in the weld metal by sizes are absent, which would allow performing the corresponding numerical forecasts, although the urgency of possibility of such forecasts is undoubted.

PROCEDURE OF WORK

Digital images of the surface of non-etched sections were obtained in the NEOPHOT-30 optical microscope with the use of a high-resolution digital camera. Further images were processed in order to increase the accuracy of a further recognition of non-metallic inclusions by means of the special software (Gaussian filter was used [12]). The size of each image amounts to 2592 by 1944 pixels. Processed images were subjected to recognition with the use of the special software (trial version of Media Cybernetics ImagePro, available on the site of the manufacturer http://www.mediacy.com/). According to this methodology, the volumetric content ($V_{\text{nm.inc}}$) and distribution of non-metallic inclusions in the weld metal was determined.

Consideration of the nature of distribution of non-metallic inclusions was started from the model (1), found for the processes of steel making. The value of the parameter n_0 for the conditions of weld pool existence can be determined based on the law of conservation of a substance based on such considerations:

The amount of oxygen in the inclusion of radius r and density ρ_{inc} is equal to $\frac{4}{3}\pi r^3 \rho_{\text{inc}} X_{\text{O}}$, where X_{O} is the mass fraction of oxygen in the inclusion. Then, according to the expression (1), the amount of oxygen in the inclusions of radius r is equal to

$$\frac{4}{3}\pi r^3 \rho_{\text{inc}} X_{\text{O}} n(r) = \frac{4}{3}\pi \rho_{\text{inc}} X_{\text{O}} n_0 e^{-\lambda r} r^3.$$

Consequently, the total amount of oxygen contained in the inclusions with the radius ranging from $r_{\min}$ to $r_{\max}$ is determined by the integral

$$\frac{4}{3}\pi \rho_{\text{inc}} X_{\text{O}} n_0 \int_{r_{\min}}^{r_{\max}} r^3 e^{-\lambda r} dr. \tag{2}$$

On the other hand, having marked density of molten steel by ρ_s, and the content of oxygen in the inclusions for the unit of a molten metal mass by w_{O}, the mentioned amount of oxygen in the inclusions can be evaluated by the product $\rho_s w_{\text{O}}$, which, according to the law of conservation of a substance, should be equated to the expression (2):

$$\frac{4}{3}\pi \rho_{\text{inc}} X_{\text{O}} n_0 \int_{r_{\min}}^{r_{\max}} r^3 e^{-\lambda r} dr = \rho_s w_{\text{O}}.$$

From the last equality we obtain an expression for the parameter n_o:

$$n_0 = \frac{3\rho_s w_{\text{O}}}{4\pi \rho_{\text{inc}} X_{\text{O}} \int_{r_{\min}}^{r_{\max}} r^3 e^{-\lambda r} dr}. \tag{3}$$

In order to simplify the work with the expression (3), following [12], w_{O} can be replaced in it by [O%], i.e., the total amount of oxygen in molten metal. Such a replacement means that further results on the number of inclusions will actually provide the upper limit of numerical evaluation.

In addition, the integral in the denominator of the fraction from the expression (3) can be calculated exactly, as far as according to [13]

$$\int x^3 e^{ax} dx = e^{ax}\left(\frac{x^3}{a} - \frac{3x^2}{a^2} + \frac{6x}{a^3} - \frac{6}{a^4}\right),$$

from which it follows that

Table 1. Chemical composition and content of non-metallic inclusions in the weld metal

Weld number	Mass fraction (%) in the weld metal												V_{nmincl}, %
	C	Si	Mn	S	P	Cr	Ni	Mo	Cu	Al	Ti	O	
NN1	0.034	0.212	1.51	0.023	0.021	0.41	3.74	0.44	0.12	0.022	0.009	0.078	0.62
NN2	0.038	0.417	1.57	0.025	0.022	0.33	3.50	0.52	0.13	0.034	0.044	0.070	0.58
NN3	0.034	0.321	1.38	0.023	0.015	0.39	3.83	0.51	0.12	0.020	0.005	0.067	0.55
NN4	0.050	0.290	1.32	0.024	0.014	0.16	2.19	0.27	0.36	0.039	0.019	0.061	0.47
NN5	0.049	0.298	1.39	0.023	0.015	0.15	2.26	0.25	0.44	0.039	0.008	0.072	0.58

$$\int_{r_{\min}}^{r_{\max}} r^3 e^{-\lambda r} dr =$$

$$= \frac{1}{\lambda}\left[\exp\left(-\lambda r_{\max}\right) r_{\max}^3 - \exp\left(-\lambda r_{\min}\right) r_{\min}^3\right] -$$
$$-\frac{3}{\lambda^2}\left[\exp\left(-\lambda r_{\max}\right) r_{\max}^2 - \exp\left(-\lambda r_{\min}\right) r_{\min}^2\right] + \quad (4)$$
$$+\frac{6}{\lambda^3}\left[\exp\left(-\lambda r_{\max}\right) r_{\max} - \exp\left(-\lambda r_{\min}\right) r_{\min}\right] -$$
$$-\frac{6}{\lambda^4}\left[\exp\left(-\lambda r_{\max}\right) - \exp\left(-\lambda r_{\min}\right)\right].$$

Taking into account the fact that the values of the smallest and largest radii of inclusions differ by at least an order of value, it is possible to obtain a simple approximate numerical evaluation by a further replacement of a finite integral to an infinite one in the interval (from 0 to ∞) in the expression (3), then, according to [13]:

$$\int_0^{\infty} r^3 e^{-\lambda r} dr = \frac{6}{\lambda^4}$$

and, therefore

$$n_0 = \frac{1}{8\pi} \frac{\rho_s [\text{O\%}]}{\rho_{\text{inc}} X_{\text{O}}} \lambda^4. \quad (5)$$

The relative error of calculation according to the formula (5) is lower than 2.4 % as compared to the calculation by exact quadrature (4).

OBTAINED RESULTS

In order to check the suitability of the distribution modeling according to the formula (1), experimental studies were performed, where the characteristics of non-metalic inclusions in the weld metal were determined, which differed in the time of existence of the liquid metal of the welding pool depending on the input energy of the process as well as its chemical composition. The specimens of the deposited metal, produced in submerged arc welding of butt joints of low-alloy steel 10KhSND of 14 mm thickness with an input energy of 36 kJ/cm (welds NN-1, NN-2, NN-3), as well as in a shielding gas with an input energy of 21 kJ/cm (welds NN-4, NN-5), were subjected to examination. The parameters of the welding mode meet the requirements of the standards ISO 14171 (submerged arc welding) and ISO 26304 (welding in a shielding gas). The chemical composition of the metal of welds and their content of non-metallic inclusions ($V_{\text{nm.inc}}$) are given in Table 1. Other features of the procedure of experimental investigations are presented in [13].

Our experimental study of distribution of non-metallic inclusions in the metal of welds produced by the methods of submerged arc and flux-cored wire welding (Figure 1) showed that experimental distributions are not exponential with a reliable probability of at least 95 % according to Pearson and Kolmogorov-Smirnov criteria.

Analytical analysis showed that the available experimental data can be described by the gamma-distribution function with a set reliable probability.

To analyze the distribution of non-metallic inclusions, the density function of the gamma-distribution probability was used, which has the form [13]

$$f(x;\alpha,\beta) = \frac{x^{\alpha-1}\exp\left(-\frac{x}{\beta}\right)}{\beta^{\alpha}\Gamma(\alpha)}, \quad (6)$$
$$\alpha,\beta > 0; \quad 0 < x < \infty,$$

where Γ(α) is the gamma function; parameters α and β are called shape and scale parameters, respectively.

This distribution is characterized by the fact that many other distributions are its partial cases. In particular, as is seen from the formulas (6) and (1), provided that the parameter of the shape $\alpha = 1$, the gamma-distribution is converted into an exponential distribution. Moreover, in the case of increase in the value of the shape parameter, the distribution behaviour changes qualitatively (Figure 2).

Analysis of the behaviour of the probability density functions of exponential and gamma-distribution, as well as the physical phenomenon of coarsening non-metallic inclusions due to coagulation leads to the following model description of the distribution of non-metallic inclusions in the weld metal.

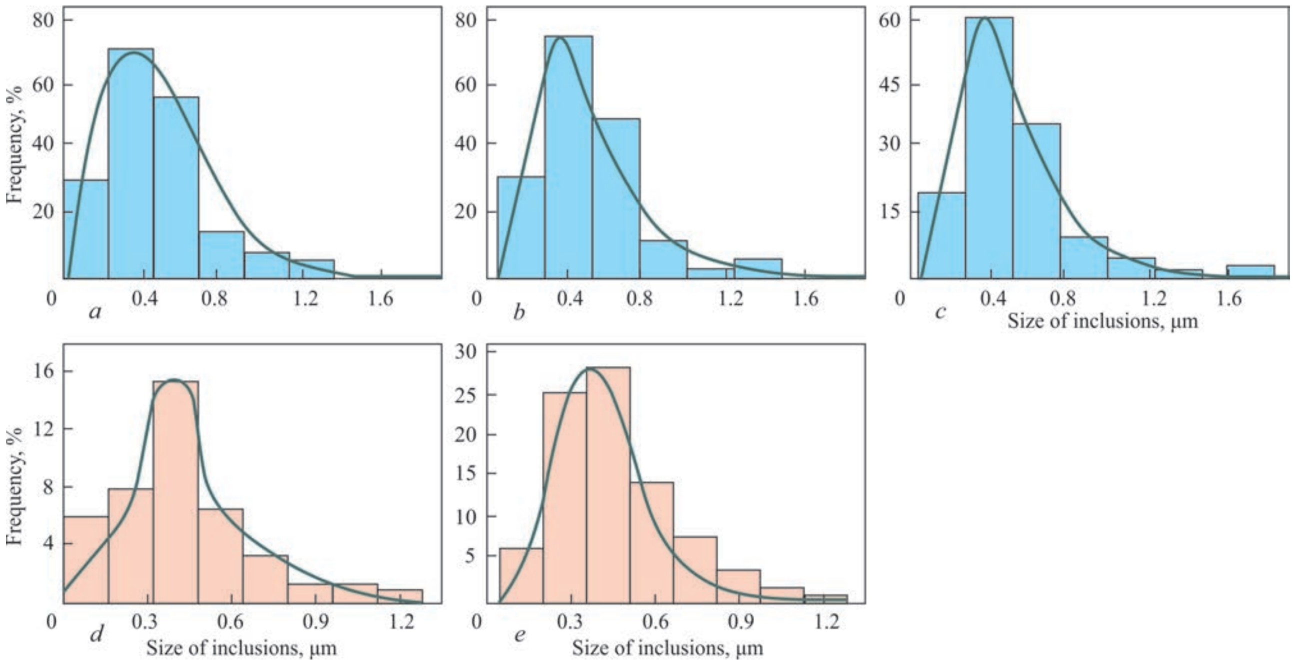

Figure 1. Histograms of distribution of non-metallic inclusions by sizes according to the results of submerged arc welding and corresponding calculated curve of probability density function according to the gamma-distribution: *a–c* — input energy of welding 36 kJ/cm; *d, e* — 21; *a* — weld NN1; *b* — NN2; *c* — NN3; *d* — NN4; *e* — NN5

At the beginning of the process of coarsening non-metallic inclusions, their distribution by sizes is subjected to the exponential law, since the vast majority of them have small radii close to the critical.

In the process of coarsening due to coagulation, a relative number of inclusions of small radii decreases, and large — increases, which leads to the change in the shape of the distribution function from a monotonically descending one, corresponding to the exponential distribution by sizes, to a single-modal one (with the maximum), corresponding to the gamma-distribution.

Thus, at the moment of beginning of the process (time variable $t = 0$), the shape parameter $\alpha = 1$, and at the end of the process, according to our experimental and calculation data, it acquires a value from the range of 2.33–4.15 (Table 2).

Denoting the final value of the shape parameter by α_k and considering the shape parameter as a linear function of time $\alpha(t)$, we obtain the following dependence of the shape parameter on time:

$$\alpha(t) = \frac{\alpha_k - 1}{t_k} t + 1, \tag{7}$$

where t_k is the final value of time.

Therefore, for further evaluation calculations to analyze the distribution of non-metallic inclusions by the size in submerged arc welding, the value $\alpha_k =$ $= 3$ can be set, which is approximately the average point of the interval of changing the shape parameter in this case.

Let us assume the duration of the process under the specified welding conditions as $t_k = 3.5$ s, which follows from the results of modeling the growth of non-metallic inclusions in the weld pool metal.

Then, from the equation (7) the following equation follows to describe the dependence of the shape parameter on time:

$$\alpha(t) = \frac{4}{7} t + 1. \tag{8}$$

As far as the nucleus of the formed non-metallic inclusions are the nuclei of refractory oxides of the chemical composition $A1_2O_3$, we should further use the following values: density of steel $\rho_s = 7.15\cdot10^3$ kg/m^3; density of non-metallic inclusion (equal to the density of alumina) $\rho_{inc} = 3.97\cdot10^3$ kg/m^3; $X_O = 47.1$ % of the total amount of oxygen in the molten metal [O%] = 0.055.

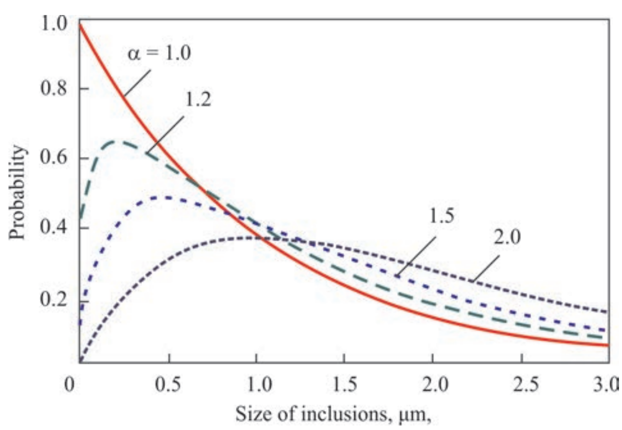

Figure 2. Change in behaviour of the gamma-distribution probability density function depending on the value of shape parameter α

Table 2. Experimental values of shape and scale parameters for submerged arc welding

Measurement code	NN1-1	NN1-2	NN1-3	NN1-4	NN1-5
Shape parameter	3.52979	2.90481	3.00837	2.81644	2.66076
Scale parameter, 10^{-6} m	7.40262	6.53177	6.51605	5.73114	4.94883
Measurement code	NN2-1	NN2-2	NN2-3	NN2-4	NN2-5
Shape parameter	2.99376	3.25676	3.19255	3.41001	2.68183
Scale parameter, 10^{-6} m	5.39726	5.99253	6.24691	6.57369	4.99286
Measurement code	NN3-1	NN3-2	NN3-3	NN3-4	NN3-5
Shape parameter	2.65562	3.30154	3.63677	3.4343	3.17487
Scale parameter, 10^{-6} m	5.12298	6.35464	6.36239	6.75384	5.51374
Measurement code	NN4-1	NN4-2	NN4-3	NN4-4	NN4-5
Shape parameter	3.94454	2.88799	2.74705	3.44743	2.33062
Scale parameter, 10^{-6} m	8.89796	5.50171	6.3869	7.40532	4.2632
Measurement code	NN5-1	NN5-2	NN5-3	NN5-4	NN5-5
Shape parameter	2.60281	4.14994	3.6945	3.54269	3.40696
Scale parameter, 10^{-6} m	548739.	8.26347	7.54531	7.70252	7.81811

Note. Shape and scale parameter was calculated by the formulas (7) and (13), respectively.

Then, the expression (5) takes the form

$$n_0 = \frac{1}{8 \cdot 3.1415926} \cdot \frac{7.15 \cdot 10^3 \cdot 0.02}{3.97 \cdot 10^3 \cdot 47.1} \lambda^4 = \\ = 0.83677 \cdot 10^{-4} \lambda^4. \tag{9}$$

Obviously, the value inverse to λ in the expression (1) is exactly a scale parameter. Therefore, let us rewrite β = 1/λ in the entered symbols and the equation (1)

$$n(r) = n_0 \exp\left(-\frac{r}{\beta}\right) = n_0 \beta \frac{1}{\beta} \exp\left(-\frac{r}{\beta}\right) = \\ = n_0 \beta f(x; 1, \beta), \tag{10}$$

from which it follows for the set values of parameters:

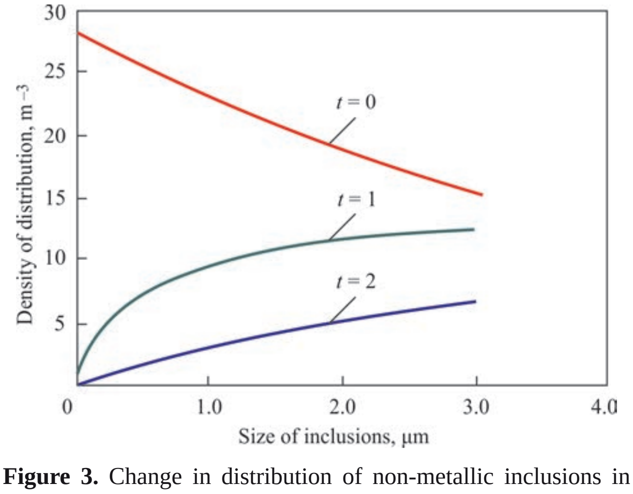

Figure 3. Change in distribution of non-metallic inclusions in time t in the conditions of lack of the formation of new nuclei of inclusions during the process

$$n(r) = 0.30428 \cdot 10^{-4} \lambda^3 f\left(x; 1, \lambda^{-1}\right) = \\ = 0.83677 \cdot 10^{-4} \beta^{-3} f(x; 1, \beta). \tag{11}$$

Dependence (11) describes the initial distribution of non-metallic inclusions in submerged arc welding by size. It is naturally that the dependence of the desired distribution on time is given in the form:

$$n(r,t) = 0{,}83677 \cdot 10^{-4} \beta^{-3} f\left(x; \alpha(t), \beta(t)\right), \tag{12}$$

where we will also consider the scale parameter as a linear function on time with finite values, corresponding to the values of the shape parameter from Table 1:

$$\beta(t) = \beta_0 + \frac{\beta_k - \beta_0}{t_k} t. \tag{13}$$

The obtained formulas allow using a tool of electron tables to calculate the distribution of non-metallic inclusions in a discrete volume of metal by sizes depending on time (Figure 3). The results shown in the diagram correspond to the data of [11].

Considering the real process, it is necessary, as is noted in [9], to take into account the formation of nuclei of non-metallic inclusions at a certain temperature depending on the rate of their formation and time spent in a set temperature range. Thus, the evaluation of the distribution density of non-metallic inclusions is obtained as the sum of products of the mentioned rates by the corresponding values of the time variable.

The final result is presented in Figure 3. It is seen that the gamma-distribution provides an objective description of the density function of the probability of distribution of non-metallic inclusions by sizes independent of the time of existence of the liquid metal in the welding pool and the chemical composition of the molten metal.

CONCLUSIONS

1. It was established that processing of experimental data on the sizes of non-metallic inclusions in the metal of welds deposited by submerged arc and shielding gas welding, showed that the final distribution of the studied inclusions by sizes is subjected to the law of gamma-distribution (probability is > 95 %).

2. It is shown that to describe the evolution of distribution of non-metallic inclusions during weld formation, it is advisable to use a probability model in the form of gamma-distribution with time-dependent parameters.

3. At the beginning of the process, the distribution of non-metallic inclusions in the proposed model is exponential due to the fact that the value of the shape parameter is equal to one. The values of the shape and scale parameters, calculated from the experimental data, are 2.6–3.9 and 4200–8900, respectively, regardless of the type of welding.

REFERENCES

1. Oh, Y.J., Lee, S.Y., Byun, J.S. et al. (2000) Non-metallic inclusions and acicular ferrite in low carbon steel. *Materials Transact., JIM*, 41(**12**), 1663–1669.
2. Quintana, M.A., McLane, J., Babu, S.S., David, S.A. (2001) Inclusion formation in self-shielded flux cored arc welds. *Welding J.*, **4**, 98–105.
3. Babu, S.S. (2004) The mechanism of acicular ferrite in weld deposits. *Current opinion in solid state and materials science*, **8**, 267–278.
4. Lee, T.K., Kim, H.J., Kang, B.Y., Hwang, S.K. (2000) Effect of inclusion size on the nucleation of acicular ferrite in welds. *ISIJ Int.*, 40(**12**), 1260–1268.
5. Zhang, J., Lee, H.G. (2004) Numerical modeling of nucleation and growth of inclusions in molten steel based on mean processing parameters. *Ibid.*, 44(**10**), 1629–1638.
6. Kwon, Y.-J., Zhang, J., Lee, H.-G. (2008) A CFD-based nucleation-growth-removal model for inclusion behavior in a gas-agitated ladle during molten steel deoxidation. *Ibid.*, 48(**7**), 891–900.
7. Njzawa, H., Kato, Y., Sorimachi, K., Nakanishi, T. (1999) Agglomeration and flotation of alumina clusters in molten steel. *Ibid.*, 39(**5**), 426–434.
8. Zinngrebe, E., Van Hoek, C., Visser, H. et al. (2012) Inclusion population evolution in Ti-alloyed Al-killed steel during secondary steelmaking process. *Ibid.*, 52(**1**), 52–61.
9. Hong, T., Debroy, T., Babu, S.S., David, S.A. (2000) Modeling of inclusion growth and dissolution in the weld pool. *Metallurgical and Materials Transact.: B., 20B*, **2**, 161–169.
10. Zhang, L., Thomas, B.G. (2003) Inclusion nucleation, growth, and mixing during steel deoxidation. UIUC. *Continuous Casting Report,* **200206**, 1–19.
11. Zhang, B.W., Li, B.W. (2007) Growth kinetics of single inclusion particle in molten melts. *Acta Metallurgica Sinica*, 20(**2**), 129–138.
12. *Lucas J.* van Vliet, Ian T. Young, Piet, W. (1998) Verbeek Recursive Gaussian Derivative Filters Fac. of Appl. Phys., Delft Univ. of Technol. DOI: 10.1109/ICPR.1998.711192. Conference: Pattern Recognition. In: *Proc. of Fourteenth Int. Conf.*, Vol. 1.
13. Gradshtejn, I.S., Ryzhik, I.M. (1971) *Tables of integrals, sums, series and products*. Moscow, Nauka [in Russian].
14. Golovko, V.V., Pokhodnya, I.K. (2013) Effect of non-metallic inclusions on formation of structure of the weld metal in high-strength low-alloy steels. *The Paton Welding J.*, **6**, 2–10.

ORCID

V.V. Holovko: 0000–0002–2117–0864

CONFLICT OF INTEREST

The Authors declare no conflict of interest

CORRESPONDING AUTHOR

V.V. Holovko

E.O. Paton Electric Welding Institute of the NASU

11 Kazymyr Malevych Str., 03150, Kyiv, Ukraine

E-mail: v_golovko@ukr.net

SUGGESTED CITATION

L.A. Taraborkin, V.V. Holovko (2021) Calculated-experimental model of distribution of non-metallic inclusions in the metal of welds by sizes. *The Paton Welding J.*, **12**, 18–23. https://doi.org/10.37434/tpwj2021.12.03

JOURNAL HOME PAGE

https://pwj.com.ua/en

Received 12.10.2021

Accepted: 24.12.2021

DECEMBER 22, 2007 French carrier rocket Ariane 5 launched the first ever African satellite. To create Ariane 5, the engineers supervising welding of the fuel tank for the rocket, made it from aluminium 3 mm thick. The welding unit was rotating inside the tank that allowed conducting seamless welding. The weld integrity is of critical importance, as cryogenic tanks form the load-carrying structure of the carrier rocket first stage. In addition, KUKA welding robots were used to build the rocket, which also ensured seamless welding.